Multipore membranes with nanofluidic diodes allowing multifunctional rectification and logical responses

Javier Cervera, Patricio Ramirez, Vicente Gomez, Saima Nasir, Mubarak Ali, Wolfgang Ensinger, Pieter Stroeve, and Salvador Mafe

Articles you may be interested in

Field effect modulated nanofluidic diode membrane based on Al2O3/W heterogeneous nanopore arrays
Appl. Phys. Lett. **102**, 213108 (2013); 10.1063/1.4807781

Information processing with a single multifunctional nanofluidic diode
Appl. Phys. Lett. **101**, 133108 (2012); 10.1063/1.4754845

Effect of surface charge density and electro-osmotic flow on ionic current in a bipolar nanopore fluidic diode
J. Appl. Phys. **110**, 084322 (2011); 10.1063/1.3656708

Ion current rectification in a fluidic bipolar nanochannel with smooth junction
Appl. Phys. Lett. **99**, 113103 (2011); 10.1063/1.3627181

Electrolyte diodes with weak acids and bases. I. Theory and an approximate analytical solution
J. Chem. Phys. **123**, 164509 (2005); 10.1063/1.2085047

Multipore membranes with nanofluidic diodes allowing multifunctional rectification and logical responses

Javier Cervera,[1] Patricio Ramirez,[2,a)] Vicente Gomez,[2] Saima Nasir,[3] Mubarak Ali,[3,4] Wolfgang Ensinger,[3] Pieter Stroeve,[5] and Salvador Mafe[1]

[1]*Dept. de Física de la Terra i Termodinàmica, Universitat de València, E-46100 Burjassot, Spain*
[2]*Dept. de Física Aplicada, Universitat Politècnica de València, E-46022 València, Spain*
[3]*Department of Material- and Geo-Sciences, Materials Analysis, Technische Universität Darmstadt, D-64287 Darmstadt, Germany*
[4]*Materials Research Department, GSI Helmholtzzentrum für Schwerionenforschung, Planckstrasse 1, D-64291 Darmstadt, Germany*
[5]*Department of Chemical Engineering, University of California Davis, Davis, California 95616, USA*

We have arranged two multipore membranes with conical nanopores in a three-compartment electrochemical cell. The membranes act as tunable nanofluidic diodes whose functionality is entirely based on the pH-reversed ion current rectification and does not require specific surface functionalizations. This electrochemical arrangement can display different electrical behaviors (quasi-linear ohmic response and inward/outward rectifications) as a function of the electrolyte concentration in the external solutions and the applied voltage at the pore tips. The multifunctional response permits to implement different logical responses including *NOR* and *INHIBIT* functions. *Published by AIP Publishing.* [http://dx.doi.org/10.1063/1.4954764]

Microfluidic functionality is often achieved by externally tuning the interaction between free ions in solution and immobilized charged groups on the pore surface. The wide range of surface functionalizations currently available for biologically oriented sensors and actuators tuned by different chemical, thermal, electrical, and optical signals[1–7] is remarkable. Practical applications are, however, limited by the high variability observed in the individual nanostructure responses and the continuous operation after several cycles. In those cases where a reliable electrical response rather than a highly specific analyte recognition[5,8–10] is required, these problems can be circumvented by using multipore membranes with multifunctional fixed charge groups showing a high stability.

We have arranged two multipore membranes with conical nanopores of different electrical signs in a three-compartment cell and showed that the resulting electrochemical circuitry permits additional levels of functionality. The individual nanofluidic diodes show pH-reversed ion current rectification because of the charge polarity reversal observed in the acidic groups anchored to the pore surface. The membranes can display different electrical behavior (quasi-linear resistor and diode-like inward/outward rectifications) as a function of the electrolyte concentration and pH in the external solutions and the applied voltage at the pore tips. Thus, the membrane performance is entirely based on the pH-reversed ion current rectification[11] and does not require highly specific functionalizations of the pore surface.[3,12]

The multifunctional response is robust enough to permit different logical functions including *NOR* and *INHIBIT* gates, which are of current interest for liquid state transducers and actuators.[3,13–16] The *NOR* gate is functionally complete and the *INHIBIT* function is difficult to implement in practice

because it should give the output "1" only for one particular combination of inputs "0" and "1." While this requirement may be fulfilled by using three rather than two inputs and particular combinations of two of the basic functions,[17] we have used here only two inputs.

Stacks of six polyimide foils 12.5-μm thick (Kapton50 HN, DuPont) were irradiated under normal incidence with single uranium ions of energy 11.4 MeV per nucleon at the linear accelerator UNILAC (GSI, Darmstadt). The range of the ions in polyimide under these conditions was larger than the thickness of the foil stack and the energy loss of the ions was well above the threshold required for homogeneous track etching. A metal mask with a centered aperture of diameter 200 μm was placed in front of each stack for single-ion irradiation. The ion beam was blocked promptly as soon as a single ion passed through the foil stack and was registered by a particle detector behind the samples. Tracks in multipore and single pore membranes were then produced. The tracks were used to create approximately conical pores by means of asymmetric track-etching.[18] The pore radii were estimated from SEM and the steady-state current (I)–potential (V) curves to be in the ranges 300–600 nm (base) and 10–40 nm (tip). The membrane areas exposed to the solutions were approximately 1 cm^2. The multipore membranes have pore densities of approximately 10^4 pores/cm^2. The etching process gave carboxylate residues on the pore wall surface. The residues were in ionized form at pH = 7. The solution pH was monitored by a Crison GLP22 pH-meter before and after each measurement.

Input voltages were applied with Ag|AgCl electrodes immersed in the bathing solutions at ambient temperature. The electric potential is asymmetric along the pore axis because of the conical geometry: the surface charge density is constant but the pore radius changes along the axial direction. The electrical rectification arises because the pore resistance is low when the current enters the cone tip while it

a)Author to whom correspondence should be addressed. Electronic mail: patraho@fis.upv.es

108, 253701-1

is high when the current enters the cone base.[19] The cation flow constitutes the main contribution to current at low voltages. The pores lose their selectivity for cations,[19] and then the current is carried by cations moving in the direction of the current and anions moving in opposite direction to the current, at high enough voltages. To record the I–V curves in the three-compartment electrochemical cell, a picoammeter/voltage source (Keithley 6487/E) was used.

Most experiments on conical pores conducted at pH values higher than the pK_a of the carboxylic acid groups have found significant electrical rectification ascribed to the negative charges on the pore surface due to the group deprotonation. On the contrary, decreasing the pH values leads to a decrease in the electrical rectification due to the protonation of these groups. When the solution ionic strength and pH take sufficiently low values, the rectification becomes significant again and opposes to that obtained at high pH.[11] This fact suggests that the pore surface is now positively charged. The charge reversal may occur because of further protonation of the neutral carboxylic acid or the hydrogen bonded hydrogel layer inside the nanopore.[11,20] Note also that, since the membrane material is polyamide, the imide linkages could also be protonated under acidic conditions.

Figure 1(a) shows the I–V curves obtained for a multipore membrane in a two-compartment cell at ambient temperature. The experimental data correspond to the cases of an aqueous KCl solution of concentration $c = 0.1$ M at pH = 7 (top curve) and an aqueous HCl solution of pH = 1 (bottom curve). In both cases, the membrane is flanked by two identical solutions and the voltage is applied on the electrode in the left solution (the other electrode is connected to ground). The charge asymmetry along the pore produces the electrical rectification found in Fig. 1(a). Indeed, no electrical rectification is observed in control experiments conducted at intermediate pH values because the acidic groups on the pore surface are in neutral form.[19] Previous studies on nanofluidic diodes[21–23] have demonstrated that the diode functionality depends critically on the pH-regulated pore surface charge.

For the KCl solution curve of Fig. 1(a), the electrical resistance is low for $V > 0$: the current enters the cone tip with a high concentration of positive mobile ions compensating for the high and negative fixed charge density. On the contrary, this resistance is high for $V < 0$: the current enters now the cone base with a low charge density.[18] Note that the opposite behavior is obtained for the HCl solution curve, suggesting that this reverse rectification is now due to positive fixed charges on the pore surface. The currents obtained at high voltages are higher in the HCl than in the KCl solution because of the high hydrogen ion mobility compared with that of potassium ion. Although the exact distribution of active groups on the pore tip surface is unknown, continuum theoretical approaches assuming homogeneous surface charge densities have been able to describe the experimental results[19,24] because the tip pore radii are in the range of nanometers while typical ions (e.g., K^+) and fixed charge groups (e.g., COO^-) have much smaller diameters. In the case of pore diameters smaller than the characteristic Debye length, the continuous approach may fail and ionic size effects need to be taken into account.[25–27]
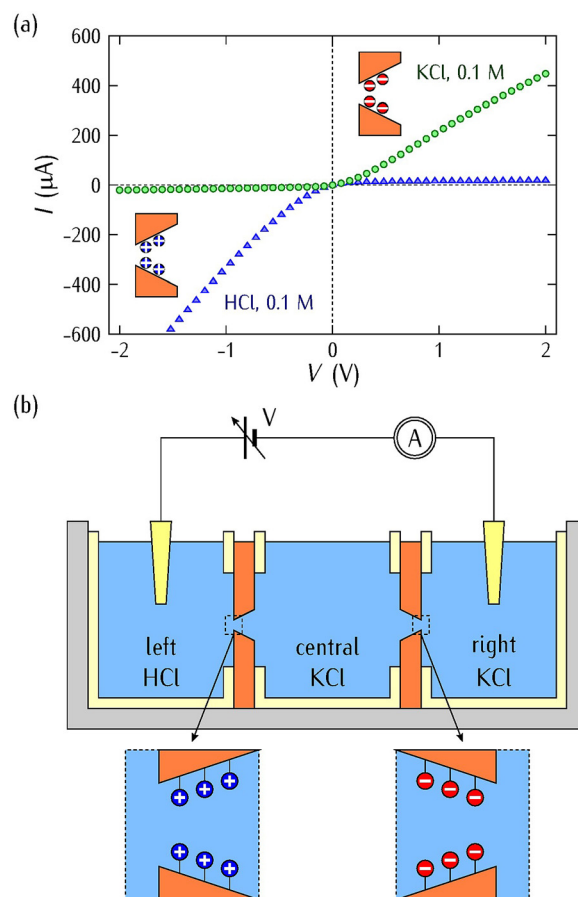

FIG. 1. (a) I–V curves obtained for a multipore membrane in a two-compartment cell for the cases of an aqueous KCl solution of concentration $c = 0.1$ M at pH = 7 (top curve) and an aqueous HCl solution of pH = 1 (bottom curve). The membrane is flanked by two identical solutions and the voltage is applied on the electrode in the left solution (the other electrode is connected to ground). (b) The three-compartment cell used in the experiments with two multipore membranes arranged in series. All nanofluidic diodes in the multipore membranes have their functionalized tips exposed to the left and right solutions. A particular arrangement for the HCl and KCl solutions in the cell and the resulting fixed charges on the pore surface are shown.

The three-compartment cell used in the experiments with two multipore membranes arranged in series is shown in Fig. 1(b). Note that all nanofluidic diodes in the multipore membranes have their functionalized tips exposed to the left and right solutions. This arrangement facilitates the external independent reconfiguration of the pore tips because of the direct experimental access. The electrodes are placed on the left and right solutions and the conical pore basis of the individual diodes face the central volume of the electrochemical cell. The use of different solutions in the three volumes of the cell allows the multifunctional electrical responses.[3,28]

Figures 2(a)–2(c) show three control experiments conducted under different conditions. Fig. 2(a) is obtained with KCl solutions of concentration $c = 0.1$ M at pH = 7 in the three cell volumes. Note the expected current quasi-saturation obtained at high voltages because the effective diodes (multipore membranes here) are oppositely biased (see Fig. 1(b)). The saturation currents reflect that the membranes used have similar electrical characteristics.
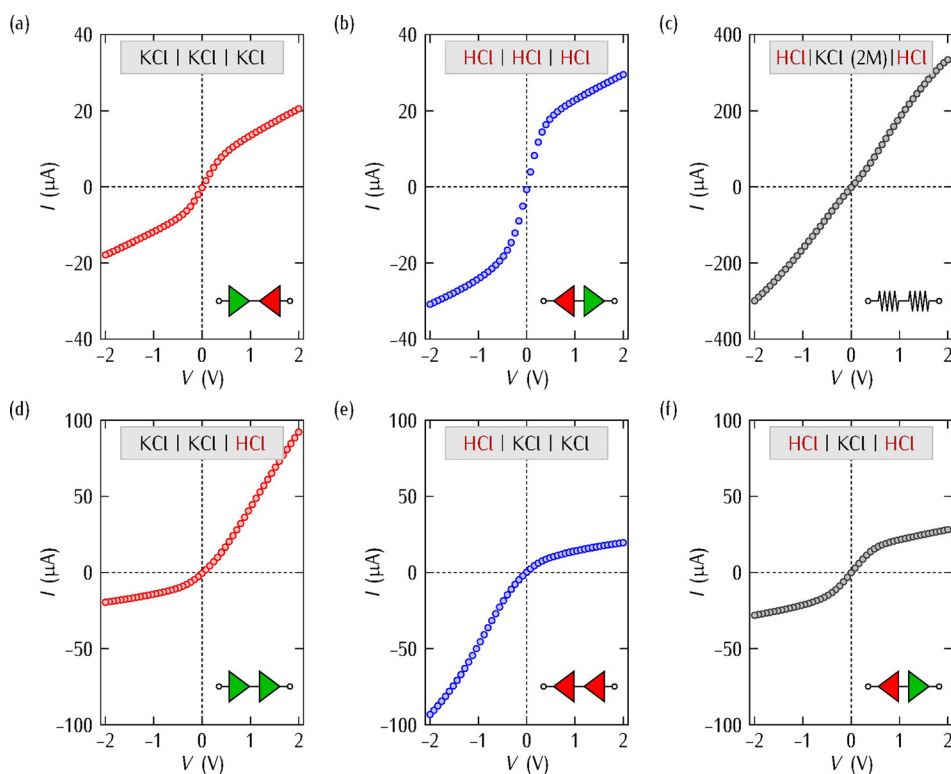
FIG. 2. *I–V* curves for the cases: (a) KCl solutions of concentration $c = 0.1$ M at pH $= 7$ in the three volumes. (b) HCl solutions at pH $= 1$ in the three volumes. (c) HCl solutions at pH $= 1$ in the left and right volumes and KCl solution of concentration $c = 2$ M at pH $= 7$ in the central volume. (d) KCl solutions of concentration $c = 0.1$ M at pH $= 7$ in the left and central volumes and HCl solution at pH $= 1$ in the right volume. (e) KCl solutions of concentration $c = 0.1$ M at pH $= 7$ in the central and right volumes and HCl solution at pH $= 1$ in the left volume. (f) HCl solutions at pH $= 1$ in the left and right volumes and KCl solution of concentration $c = 0.1$ M at pH $= 7$ in the central volume. Note the different scales in the curves. The insets schematically show the experimental conditions in the three-volume cell and the polarities of the resulting diodes. The green color corresponds to the forward polarized conducting diode while the red color corresponds to the reverse polarized conducting diode.

Figure 2(b) is obtained with HCl solutions at pH $= 1$ in the three cell volumes. Again, the currents obtained at high voltages are higher than those of Fig. 2(a) because of the higher hydrogen mobility compared with that of potassium ion.

A third control experiment is shown in Fig. 2(c) where HCl solutions at pH $= 1$ are used in the left and right volumes while a KCl solution of concentration $c = 2$ M at pH $= 7$ is fed into the central volume. As expected, this high salt concentration in the central volume gives an increase in the absolute currents due to the increase in the number of available ions. Note also the linear (ohmic) behavior obtained: the rectification effect is lost when the mobile ions at high concentration effectively screen the positive fixed charges (see Fig. 1(a), bottom curve) on the pore surface.[12]

Figures 2(d) and 2(e) show the multifunctional rectification characteristics obtained when different solutions are used in the left and right compartments. Figure 2(d) corresponds to a KCl solution of concentration $c = 0.1$ M at pH $= 7$ in the left and central volumes and HCl solution at pH $= 1$ in the right volume only. A high electrical rectification is obtained: the multipore membranes have now different fixed charges because of the distinct pH values at the respective pore tips; see Fig. 1(a). The applied pH and potential difference effectively polarize the nanofluidic diodes in the same direction (see Fig. 1(b)).

Figure 2(e) corresponds to a KCl solution of concentration $c = 0.1$ M at pH $= 7$ in the central and right volumes and HCl solution at pH $= 1$ in the left volume only. Except for the reversal in the current rectification, Fig. 2(e) shows essentially the same behavior as Fig. 2(d) because the two multipore membranes are now polarized in the direction opposite to that in Fig. 2(d).

To check further that the rectification effect is due to the distinct pore charges resulting from the externally imposed pH differences, Fig. 2(f) shows the *I–V* curve obtained when the left and right volumes contain identical HCl solutions at pH $= 1$ and the central volume is fed with a KCl solution of concentration $c = 0.1$ M at pH $= 7$. In this symmetrical case, the currents are very similar to those in Fig. 2(b).

Taken together, the results of Figs. 2(a)–2(f) demonstrate a robust multifunctional behavior in the electrical responses. Note in particular, the significant *off/on* resistance ratios obtained despite the ohmic effect of the central volume compartment. Remarkably, the different *I–V* curves in Figs. 2(a)–2(f) are obtained with the same type of multipore membrane, which does not require a highly specific pore functionalization.[3] Note also that the protein ion channels embedded in cell membranes form aqueous pores at the nanometer scale that are decorated by amphoteric groups allowing a pH-dependent functionality (see Refs. 29 and 30 for specific examples). In this sense, the broad range of electrical responses obtained in Figs. 2(a)–2(f) can be considered as biomimetic.[6,7]

As a potential application of the above results, Figs. 3(a)–3(d) show that different logical responses (*NOR* and *INHIBIT*) can be obtained using the chemical (pH) and electrical (*V*, *I*) signals in Figs. 2(a)–2(f). Figure 3(a) illustrates the general procedure followed in the respective *I–V* curves of Figs. 2(a)–2(f) for the case of the *NOR* function. The *NOR* gate (Fig. 3(b)) is functionally complete in the sense that any digital logic circuit can be built out using only *NOR* gates. The *INH*-1 (Fig. 3(c)) and 2 (Fig. 3(d)) functions are difficult to implement because they should give the output "0" in all cases except for one particular combination of inputs "0" and "1." All logic functions can be implemented
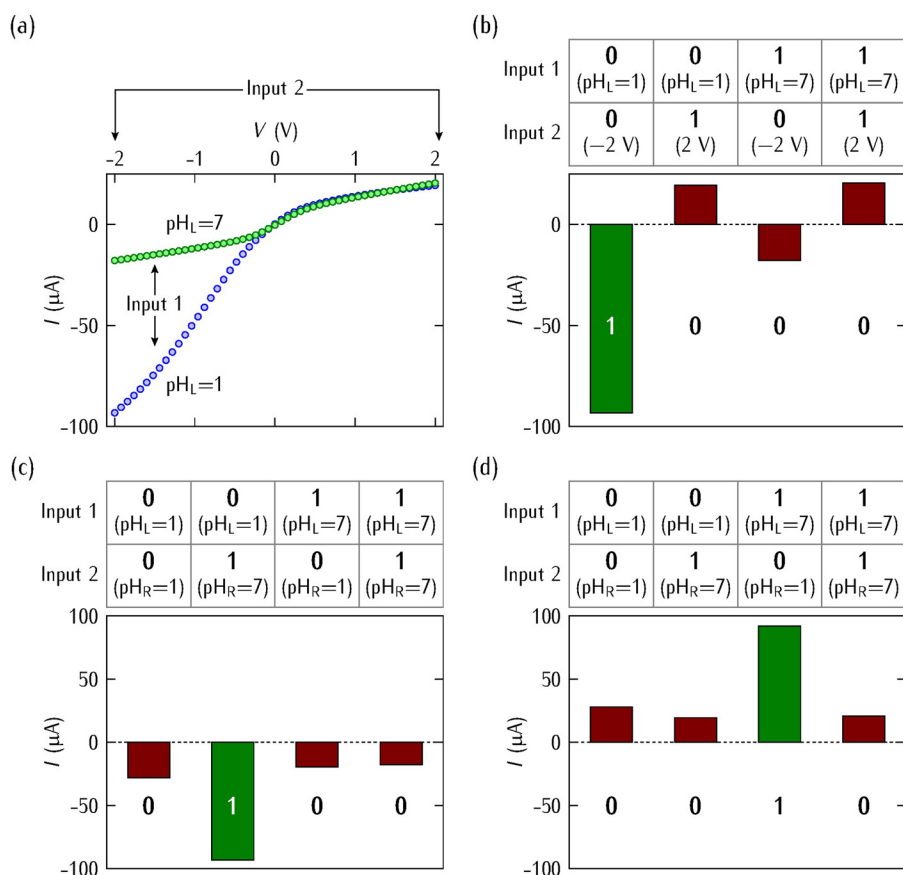
FIG. 3. (a) Scheme for the logic function in the case of the *NOR* function implemented using the *I–V* curve. (b) *NOR* (pH (right) = 7 is fixed) (c) *INHIBIT*-1 (*V* = −2 V is fixed), and (d) *INHIBIT*-2 (*V* = 2 V is fixed) logical functions obtained using the chemical (pH) and electrical (*V*, *I*) signals in Figs. 2(a)–2(f). The current is the *output* value and the tables include the respective *input* values in each case.

using the same type of membrane incorporating conical pores functionalized with carboxylic acidic groups and the three-compartment cell of Fig. 1(b). However, the logic outputs "0" and "1" are only approximately defined in our experiments because of the moderate rectification that results from the ohmic behavior of the central volume arranged in series with the two membranes (Fig. 1(b)). In principle, this rectification could be enhanced by modifying the central compartment characteristics and controlling the pore tip shape and the nature and distribution of the pH-sensitive groups.[12,23,31]

We use a three-compartment electrochemical cell and two multiporous membranes with conical nanopores arranged in series. The membrane functionality is based on the pH-reversed ion current rectification and does not require specific surface functionalizations. The externally tunable arrangement of nanofluidic diodes can display different electrical behaviors including a quasi-linear ohmic response and inward/outward rectifications as a function of the electrolyte concentration in the external solutions and the applied voltage at the pore tips. The demonstrated multifunctional behavior permits different logical responses and the cases of *NOR* and *INHIBIT* functions are discussed.

[1]C. R. Martin and Z. S. Siwy, Science **317**, 331 (2007).
[2]X. Hou and L. Jiang, ACS Nano **3**, 3339 (2009).
[3]P. Ramirez, J. Cervera, M. Ali, W. Ensinger, and S. Mafe, ChemElectroChem **1**, 698 (2014).
[4]H. Chun and T. D. Chung, Annu. Rev. Anal. Chem. **8**, 441 (2015).
[5]D. G. Haywood, A. Saha-Shah, L. A. Baker, and S. C. Jacobson, Anal. Chem. **87**, 172 (2015).
[6]M. Tagliazucchi and I. Szleifer, Mater. Today **18**, 131 (2015).
[7]H. Zhang, Y. Tian, and L. Jiang, Nano Today **11**, 61 (2016).
[8]M. Ali, S. Nasir, P. Ramirez, J. Cervera, S. Mafe, and W. Ensinger, J. Phys. Chem. C **117**, 18234 (2013).
[9]G. Pérez-Mitta, J. S. Tuninetti, W. Knoll, C. Trautmann, M. E. Toimil-Molares, and O. Azzaroni, J. Am. Chem. Soc. **137**, 6011 (2015).
[10]M. Ali, I. Ahmed, P. Ramirez, S. Nasir, C. M. Niemeyer, S. Mafe, and W. Ensinger, Small **12**, 2014 (2016).
[11]Z. Guo, J. Wang, J. Ren, and E. Wang, Nanoscale **3**, 3767 (2011).
[12]M. Ali, P. Ramirez, H. Q. Nguyen, S. Nasir, J. Cervera, S. Mafe, and W. Ensinger, ACS Nano **6**, 3631 (2012).
[13]B. E. Fratto, L. J. Roby, N. Guz, and E. Katz, Chem. Commun. **50**, 12043 (2014).
[14]P. Ramirez, M. Ali, W. Ensinger, and S. Mafe, Appl. Phys. Lett. **101**, 133108 (2012).
[15]K. Tybrandt, R. Forchheimer, and M. Berggren, Nat. Commun. **3**, 871 (2012).
[16]M. Ali, S. Nasir, P. Ramirez, I. Ahmed, Q. H. Nguyen, L. Fruk, S. Mafe, and W. Ensinger, Adv. Funct. Mater. **22**, 390 (2012).
[17]A. Prasanna de Silva, I. M. Dixon, H. Q. Nimal Gunaratne, T. Gunnlaugsson, P. R. S. Maxwell, and T. E. Rice, J. Am. Chem. Soc. **121**, 1393 (1999).
[18]P. Apel, Radiat. Meas. **34**, 559 (2001).
[19]P. Ramirez, V. Gomez, J. Cervera, S. Nasir, M. Ali, W. Ensinger, and S. Mafe, Nano Energy **16**, 375 (2015).
[20]C. F. Wells, J. Phys. Chem. **77**, 1994 (1973).
[21]I. Vlassiouk and Z. S. Siwy, Nano Lett. **7**, 552 (2007).

[22]R. Karnik, C. Duan, K. Castelino, H. Daiguji, and A. Majumdar, Nano Lett. **7**, 547 (2007).

[23]S. Nasir, M. Ali, P. Ramirez, V. Gomez, B. Oschmann, F. Muench, M. N. Tahir, R. Zentel, S. Mafe, and W. Ensinger, ACS Appl. Mater. Interfaces **6**, 12486 (2014).

[24]J. Cervera, B. Schiedt, R. Neumann, S. Mafe, and P. Ramirez, J. Chem. Phys. **124**, 104706 (2006).

[25]F. M. Gilles, M. Tagliazucchi, O. Azzaroni, and I. Szleifer, J. Phys. Chem. C **120**, 4789 (2016).

[26]E. R. Cruz-Chu, T. Ritz, Z. S. Siwy, and K. Schulten, Faraday Discuss. **143**, 47 (2009).

[27]J. Cervera, P. Ramirez, J. A. Manzanares, and S. Mafe, Microfluid. Nanofluid. **9**, 41 (2010).

[28]L. Zeng, Z. Yang, H. Zhang, X. Hou, Y. Tian, F. Yang, J. Zhou, L. Li, and L. Jiang, Small **10**, 793 (2014).

[29]B. Hille, *Ion Channels of Excitable Membranes* (Sinauer Associates Inc., Sunderland, MA, 1992).

[30]M. Queralt-Martín, E. García-Giménez, V. M. Aguilella, P. Ramirez, S. Mafe, and A. Alcaraz, Appl. Phys. Lett. **103**, 043707 (2013).

[31]Z. Zhang, X.-Y. Kong, K. Xiao, Q. Liu, G. Xie, P. Li, J. Ma, Y. Tian, L. Wen, and L. Jiang, J. Am. Chem. Soc. **137**, 14765 (2015).